ACS APPLIED MATERIALS & INTERFACES

Research Article

www.acsami.org

Cellulose Nanofibril/Reduced Graphene Oxide/Carbon Nanotube Hybrid Aerogels for Highly Flexible and All-Solid-State Supercapacitors

Qifeng Zheng,[†] Zhiyong Cai,[‡] Zhenqiang Ma,[§] and Shaoqin Gong*[,†]

[†]Department of Biomedical Engineering, Material Science Program, and Wisconsin Institute for Discovery, University of Wisconsin−Madison, Madison, Wisconsin 53715, United States

[‡]Forest Product Laboratory, United States Department of Agriculture, Madison, Wisconsin 53726, United States

[§]Department of Electrical Engineering, University of Wisconsin−Madison, Madison, Wisconsin 53706, United States

Supporting Information

ABSTRACT: A novel type of highly flexible and all-solid-state supercapacitor that uses cellulose nanofibril (CNF)/reduced graphene oxide (RGO)/carbon nanotube (CNT) hybrid aerogels as electrodes and H_2SO_4/poly(vinyl alcohol) (PVA) gel as the electrolyte was developed and is reported here. These flexible solid-state supercapacitors were fabricated without any binders, current collectors, or electroactive additives. Because of the porous structure of the CNF/RGO/CNT aerogel electrodes and the excellent electrolyte absorption properties of the CNFs present in the aerogel electrodes, the resulting flexible supercapacitors exhibited a high specific capacitance (i.e., 252 F g^{-1} at a discharge current density of 0.5 A g^{-1}) and a remarkable cycle stability (i.e., more than 99.5% of the capacitance was retained after 1000 charge−discharge cycles at a current density of 1 A g^{-1}). Furthermore, the supercapacitors also showed extremely high areal capacitance, areal power density, and energy density (i.e., 216 mF cm^{-2}, 9.5 mW cm^{-2}, and 28.4 μWh cm^{-2}, respectively). In light of its excellent electrical performance, low cost, ease of large-scale manufacturing, and environmental friendliness, the CNF/RGO/CNT aerogel electrodes may have a promising application in the development of flexible energy-storage devices.

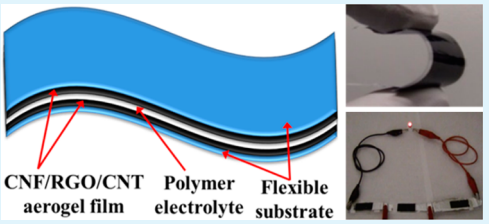

KEYWORDS: *aerogels, cellulose nanofibrils, graphene, carbon nanotube, all-solid-state supercapacitors*

INTRODUCTION

There is an increasing demand for high-performance energy-storage systems, resulting from the rapidly growing market in wearable and portable electronics such as roll-up displays and electric paper.[1−4] Lightweight, high power and energy densities, excellent durability, high flexibility, low cost, and environmental friendliness are some principal requirements of these energy-storage devices.[1,4−6] Supercapacitors, also known as electrochemical capacitors, are particularly attractive for such applications because they have high capacitances, long cycle lives, and wide working temperature ranges.[6−8] Over the past decade, a significant amount of research has been carried out to develop thin, flexible, and lightweight supercapacitors.[7−13] Nevertheless, several factors, including the high cost of raw materials and/or complicated fabrication procedures, have limited their practical applications. Therefore, there is still a need to develop high-performance supercapacitors that are based on novel, sustainable/renewable, and affordable materials.

Aerogel is a highly porous, lightweight solid material that is prepared by a process that replaces the liquid solvent in a gel with air, without substantially changing the network structure of the gel body.[14] Carbon aerogels, such as those made of graphene and carbon nanotubes, are a unique type material with high surface area, high electrical conductivity, and ultralight weight.[15] Graphene is a large single sheet of sp^2-bonded carbon that has superior electrical, optical, mechanical, and electrochemical properties.[16,17] Currently, graphene-based porous carbon materials are being extensively explored as electrode materials for supercapacitors because of their ultralow density, high specific surface area, high electrical conductivity, and good environmental compatibility.[8,13,18−24] However, one challenge with graphene is that graphene nanosheets are prone to restacking, thereby significantly limiting the diffusion of electrolyte ions.[25] Therefore, effectively preventing graphene aggregation, decreasing the ion diffusion distance, and improving the wettability of graphene by electrolytes are very important with regard to enhancing the performance of graphene-based supercapacitors.[26,27]

Cellulose is the most abundant and sustainable natural polymer.[28] Cellulose nanofibrils (CNFs) derived from cellulose have high aspect ratios, excellent mechanical properties, excellent flexibility, and superior hydrophilicity.[29,30] CNF-based aerogels possess a porous structure and an extremely high porosity (resulting in an ultralow density and a high

Received: November 14, 2014
Revised: January 14, 2015
Accepted: January 16, 2015
Published: January 27, 2015

DOI: 10.1021/am507999s
ACS Appl. Mater. Interfaces 2015, 7, 3263−3271

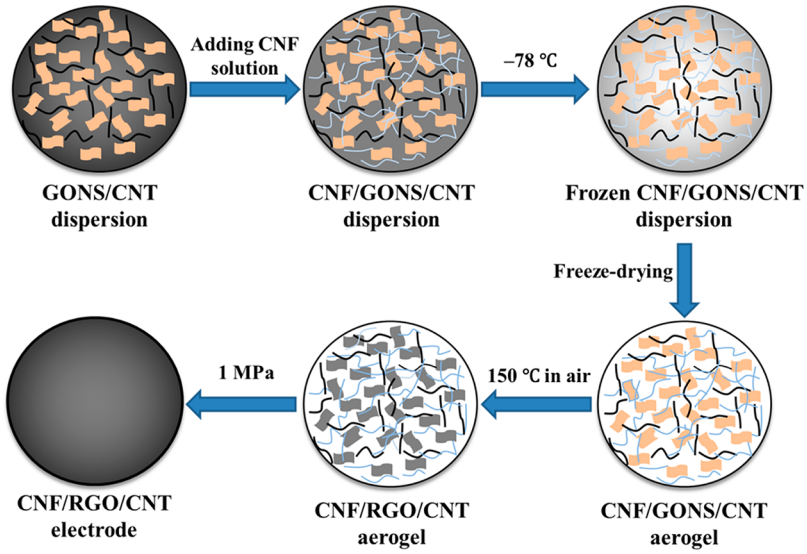

Figure 1. Schematic of the fabrication process of a CNF/RGO/CNT electrode.

specific surface area) as well as excellent electrolyte-absorption properties.[31−34] Such materials may find extensive applications in flexible energy-storage devices because CNFs can be easily integrated with conductive carbon nanofillers such as graphene and carbon nanotubes (CNTs) to achieve thin, flexible, free-standing, and binder-free high-performance flexible electrodes.[2,25,35,36] Furthermore, the hydrophilicity of CNFs in the aerogels can be beneficial for the contact between the electrodes and electrolytes and provide diffusion channels for the electrolyte ions, thus enhancing the performance of the supercapacitors.[27]

Herein, we report free-standing, lightweight, all-solid-state flexible supercapacitors fabricated by using CNF/reduced graphene oxide (RGO)/CNT hybrid aerogels as electrodes (Figure 1). Because of their high electrical conductivity, high surface area, and high mechanical strength, CNTs have attracted a lot of attention for use in supercapacitor electrode applications.[8,37,38] Graphene oxide nanosheets (GONSs) are water-soluble and have a large amount of oxygen atoms,[17] and they could easily form a uniform solution when mixed with CNFs. Furthermore, graphene oxide can be used as a surfactant to disperse the CNTs.[22,39,40] Thus, CNTs can be uniformly dispersed in the CNF/GONS aqueous solution as well.[41,42] The role of the CNTs is to provide continuous conductive paths between different layers of graphene nanosheets.[43] The resulting all-solid-state flexible supercapacitors, which use CNF/RGO/CNT aerogel sheets as electrodes, exhibit high specific capacitance and remarkable cycle stability. Furthermore, these supercapacitors also show extremely high areal capacitance, areal power density, and energy density. Therefore, we are reporting a simple and environmentally friendly method for fabricating porous electrode materials that are based on an abundant and sustainable natural polymer (i.e., CNF) and carbon materials that possess electrical and mechanical properties desirable for flexible all-solid-state supercapacitors for energy storage.

EXPERIMENTAL SECTION

Materials. CNFs were prepared using a commercially available, fully bleached eucalyptus Kraft pulp. Multiwalled CNTs (diameter = 13−16 nm) were obtained from Bayer Material Science (Pittsburgh, PA). 2,2,6,6-Tetramethyl-1-piperidinyloxy (TEMPO, 98 wt %), potassium permanganate (99 wt %), and sulfuric acid (98 wt %) were purchased from Sigma-Aldrich. Sodium chlorite, sodium bromide, phosphoric acid, and other chemicals were obtained from Fisher Scientific and used without further purification.

Preparation of CNF/RGO/CNT Aerogels. To prepare an aqueous dispersion of GONS, GONSs solid (30 mg) was dispersed in deionized water (10 mL) with the aid of sonication. CNT powder (10 mg) was added to the GONSs solution; afterward, the mixture was sonicated using a probe sonicator (UP400S, Hielscher USA) for 30 min. The resulting GONS/CNT dispersion was then added to the CNF solution (9.23 g, 0.65 wt %) under continuous magnetic stirring at room temperature to yield a homogeneous dispersion. The pH of the aqueous mixture was adjusted to neutral. The weight percentages of GONSs, CNTs, and CNFs were 30, 10, and 60%, respectively. The resulting aqueous CNF/GONS/CNF mixture was transferred into several aluminum dishes, and then frozen at −78 °C in a dry ice/acetone solution. The CNF/GONS/CNT aerogel was obtained by freeze-drying a CNF/GONS/CNT dispersion. The CNF/GONS/CNT aerogel was converted into a CNF/RGO/CNT aerogel by direct heating in an oven at 150 °C in air for 2 h.

Preparation of a H_2SO_4/Poly(vinyl alcohol)(PVA)-Gel Electrolyte.[44] In a typical process, H_2SO_4 (5 mL, 98 wt %) and PVA powder (5.0 g) were added to deionized water (50 mL). Subsequently, the whole mixture was heated to 85 °C under continuous stirring until the solution became clear.

Preparation of Flexible All-Solid-State Supercapacitors. The CNF/RGO/CNT aerogels were compressed into aerogel films under a pressure of 1.0 MPa for use as the electrodes in the supercapacitors. All compression processes described in this paragraph were carried out using a universal testing machine (Instron, model 5967) fitted with a 3 kN load. The edge of one side of the compressed aerogel film was glued to aluminum foil by using silver paste to facilitate the electrical contact of the electrode and an alligator clip connecting it to the electrochemical analyzer. Thereafter, the hot H_2SO_4/PVA-gel electrolyte (300 μL electrolyte/cm^2 of the electrode) was slowly poured onto the compressed aerogel film (10 × 25 mm^2). Next, the electrode that was coated with a thin layer of electrolyte was left in a fume hood at room temperature for about 4 h to remove the excess water by evaporation. Finally, two pieces of the resulting aerogel film that were covered by the gel electrolyte were compressed into an all-solid-state flexible supercapacitor under pressure (0.2 MPa) for 10 min. The compression force caused the electrolyte layers on each electrode merge, forming a thin separator.

Characterization and Electrical Measurement. Scanning electron microscopy (SEM, LEO GEMINI 1530) was used to characterize the microstructure of the aerogels. The thermal stability

DOI: 10.1021/am507999s
ACS Appl. Mater. Interfaces 2015, 7, 3263−3271

of these aerogels was characterized using a thermogravimetric analyzer (TGA, Q50 TA Instruments, USA) over the temperature range of 30−800 °C at a 10 °C min^{-1} heating rate under a N_2 atmosphere. Surface analysis was carried out on a K-Alpha$^+$ X-ray Photoelectron Spectrometer (XPS, Thermo Scientific, USA) with focused monochromatic Al Kα X-rays ($h\nu$ = 1286.6 eV). X-ray diffraction (XRD) patterns were measured on a D8-Discovery diffractometer (Bruker, USA) with Cu Kα radiation at a scanning rate of 5° min^{-1}. Raman spectra were studied on a DXR Raman spectrophotometer (Thermo Scientific, USA) that was equipped with a 633 nm laser source. The electrical conductivity of the CNF/RGO/CNT film was measured using an ohmmeter. To evaluate the supercapacitors, all tests were carried out using a versaSTAT-3 two-electrode system (Princeton Applied Research, USA). Specifically, cyclic voltammetry (CV) was carried out over the potential range of 0−1.0 V, galvanostatic charge−discharge was carried out over the potential range of 0−1.0 V, and electrochemical impedance spectroscopy (EIS) was carried out between 1 Hz and 100 kHz.

RESULTS AND DISCUSSION

Preparation and Characterization of CNF/RGO/CNT-Aerogel Electrodes. The fabrication process of the CNF/RGO/CNT aerogel electrodes is shown schematically in Figure 1. Previous research has demonstrated that GONSs can be used as a surfactant to disperse CNTs.[39,40] Moreover, it has also been shown that CNFs can help to disperse CNTs with the aid of sonication.[41,42] Thus, to prevent graphene aggregation effectively, GONSs and CNTs were first dispersed in the CNF solution, creating a uniform CNF/GONS/CNT dispersion. Afterward, the CNF/RGO/CNT aerogel was obtained by freeze-drying a CNF/GONS/CNT dispersion, followed by thermal reduction of GONSs in situ. Compared to the chemical reduction of GONSs, the preparation process described above excludes the use of a harmful reductive agent such as hydrazine; thus, the method aligns with the principles of green chemistry. The prepared CNF/RGO/CNT was black and ultralightweight (about 5.5 mg mL^{-1}).

Figure 2 shows the SEM images of the cryofractured surfaces of the CNF, CNF/GONS/CNT, and CNF/RGO/CNT aerogels. These aerogels all possessed a highly interconnected, 3D porous structure. The pore sizes of the CNF aerogel (Figure 2a,b; typically 4−8 μm) were somewhat larger than those of the CNF/GONS/CNT aerogel (Figure 2c,d; typically 2−5 μm). This phenomenon can be attributed to the fact that during the freeze-drying process CNTs and GONSs could easily entangle with CNFs to form a 3D network within the CNF/GONS/CNT aerogel possibly affecting the nucleation and growth of ice crystals.[42] Figure 2e,f shows the SEM images of a CNF/RGO/CNT aerogel. The 3D porous microstructure was well maintained during the thermal reduction process, and the densities of the aerogel samples were decreased to approximately 4.9 mg mL^{-1} because of the loss of oxygen-containing groups from the GONSs.

By compressing the CNF/RGO/CNT aerogel at 1 MPa, a CNF/RGO/CNT aerogel film with a thickness of approximately 200 μm was obtained. The electrical conductivity of the CNF/RGO/CNT film was 12 S m^{-1}, which is comparable to that of activated carbon (10−100 S m^{-1}).[45] The highly porous microstructure of the CNF/RGO/CNT aerogel can be largely maintained in the compressed CNF/RGO/CNT aerogel film (Figure 3a,b), although the pore diameter decreased to the nanoscale. The highly porous and nanosized microstructure of the compressed CNF/RGO/CNF aerogel film can be very helpful in increasing the absorption of the electrolytes and

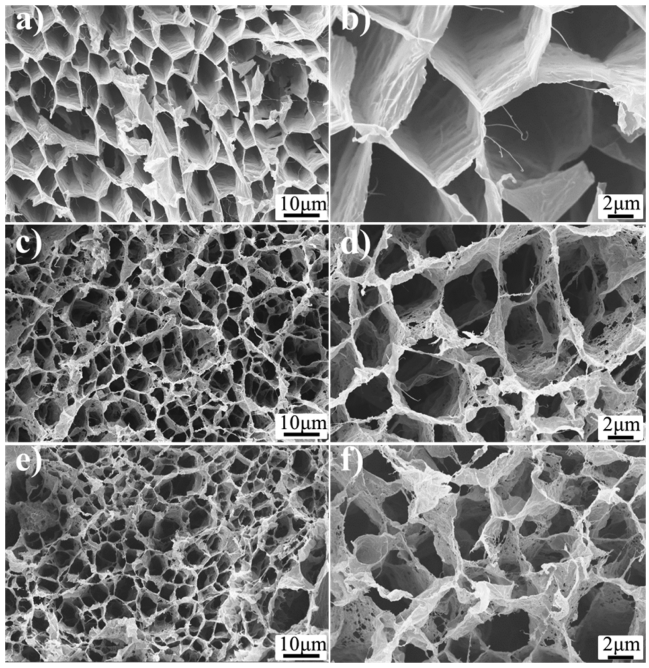

Figure 2. SEM images of the cryofractured surfaces of aerogels: (a and b) the CNF aerogel, (c and d) the CNF/GONS/CNT aerogel, and (e and f) the CNF/RGO/CNT aerogel.

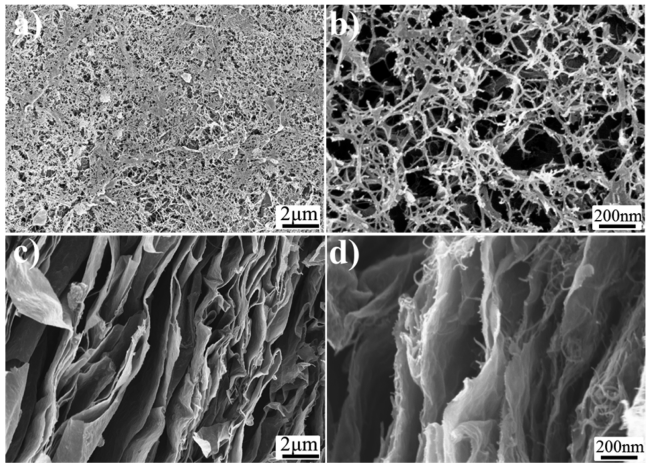

Figure 3. SEM images of the compressed CNF/RGO/CNT hybrid aerogel films: (a and b) bottom surface of the aerogel film and (c and d) cross-section of the aerogel film.

providing diffusion channels for electrolyte ions, thereby enhancing the performance of the supercapacitors. Figure 3c,d shows the cross-sectional SEM images of the compressed CNF/RGO/CNT aerogel film, from which well stacked layers can be observed.

The X-ray diffraction (XRD) patterns of the CNF, CNF/GONS/CNT, and CNF/RGO/CNT aerogels are shown Figure 4a. The XRD pattern of the CNF aerogel exhibited a distinct peak at 2θ = 22.5°, corresponding to the (002) lattice planes of cellulose I, and two overlapping peaks at 2θ = 14.0−17.8°, corresponding to the (101) and ($10\bar{1}$) lattice planes of the cellulose I crystalline structure.[32,46,47] In the XRD pattern of the CNF/GONS/CNT aerogel, a strong diffraction peak was observed at 2θ = 10.8°, corresponding to the (002) lattice planes of the graphene oxide nanosheets.[11,48] Moreover, a broad peak was observed at 2θ = 25.6°, corresponding to the

DOI: 10.1021/am507999s
ACS Appl. Mater. Interfaces 2015, 7, 3263−3271

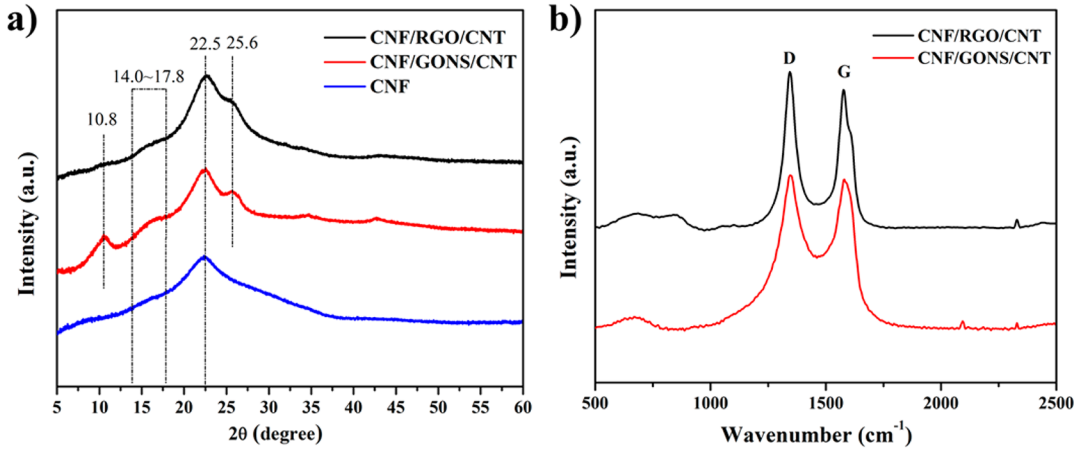

Figure 4. (a) XRD patterns of the CNF, CNF/GONS/CNT, and CNF/RGO/CNT aerogels. (b) Raman spectra of the CNF/GONS/CNT and CNF/RGO/CNT aerogels.

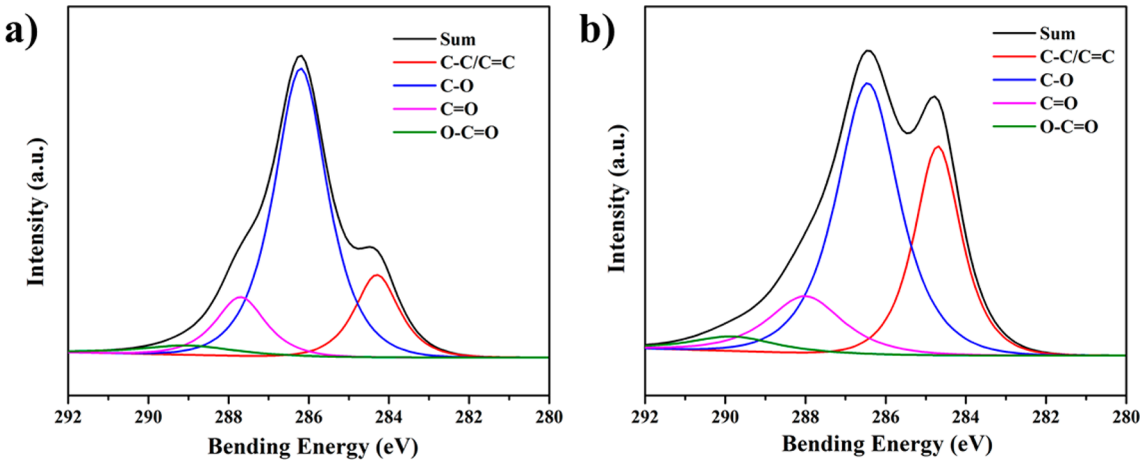

Figure 5. High-resolution XPS C1s spectra of (a) the CNF/GONS/CNT aerogel and (b) the CNF/RGO/CNT aerogel.

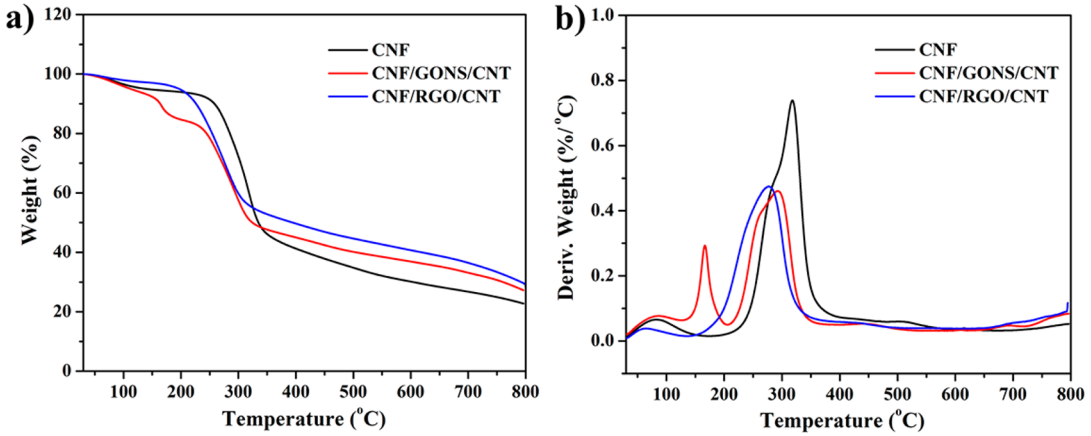

Figure 6. (a) TGA and (b) DTG curves of the CNF, CNF/GONS/CNT, and CNF/RGO/CNT aerogels.

(002) lattice planes of carbon nanotubes. However, the XRD pattern of the CNF/RGO/CNT aerogel did not show a peak at 10.8°, which indicates a high level of reduction of the graphene oxide nanosheets. Similarly, a broad peak was observed at 2θ = 25.5°, corresponding to the (002) lattice planes of reduced graphene oxide and carbon nanotubes.[49]

Raman spectroscopy was used to analyze the structural changes that occurred during the thermal reduction process of the CNF/GONS/CNF aerogel. Figure 4b shows the Raman spectra of the CNF/GONS/CNT and CNF/RGO/CNT aerogels. Two large peaks at 1348 and 1578 cm^{-1}, corresponding to the D and G bands,[50] respectively, were observed for both samples. The G band around 1578 cm^{-1} arose from the sp^2 vibration of carbon atoms in a 2D hexagonal lattice, whereas the D band arose from the sp^3 vibrations of carbon atoms of defects and disorder.[51] The intensity ratio of

DOI: 10.1021/am507999s
ACS Appl. Mater. Interfaces 2015, 7, 3263−3271

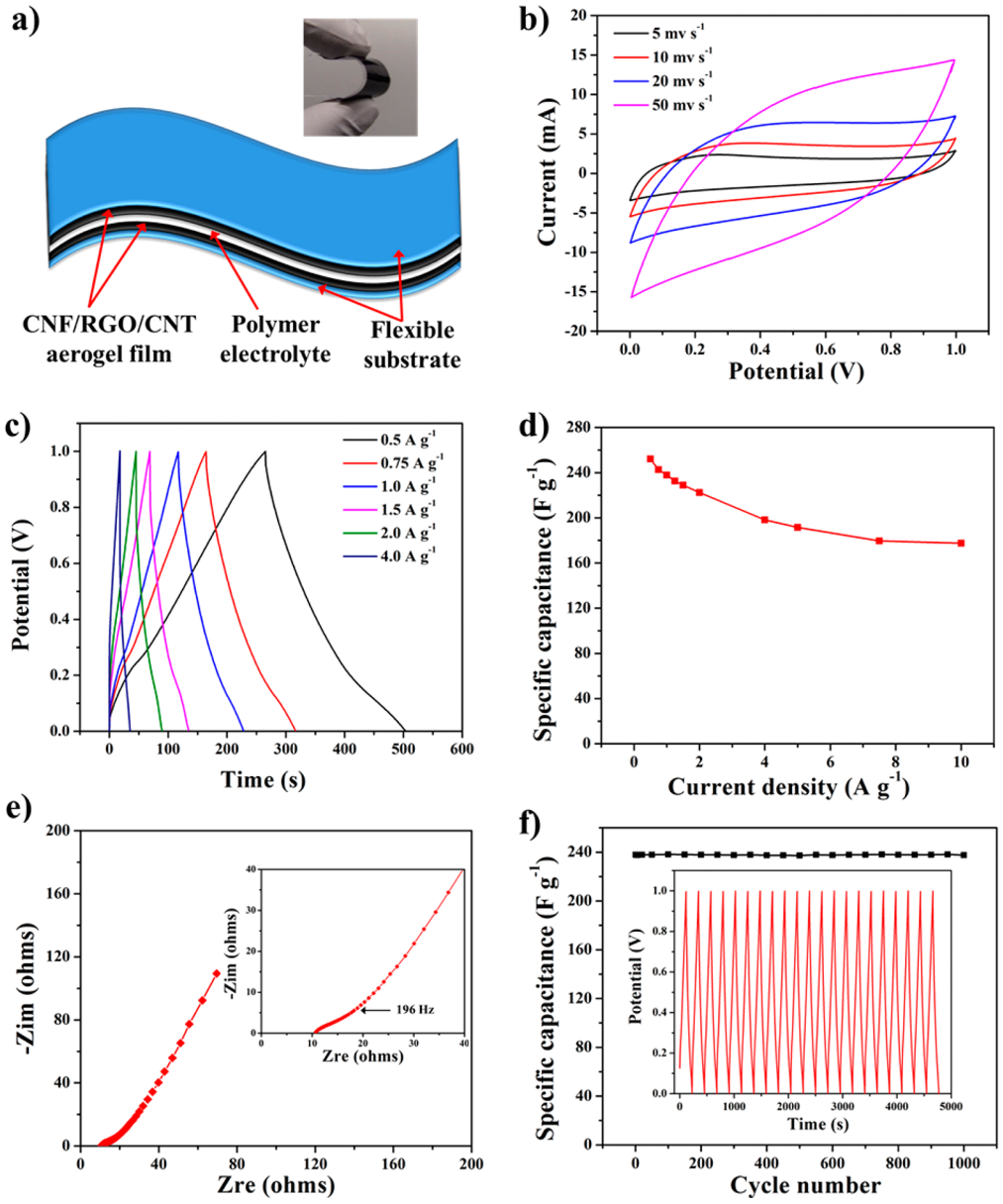

Figure 7. (a) Schematic diagram of the all-solid-state supercapacitor where the polymer-gel electrolyte serves as the electrolyte and the separator. Inset shows the flexibility of the device. (b) Typical cyclic voltammetry curves of a supercapacitor at different scan rates. (c) Charge−discharge curves of a supercapacitor at different current densities. (d) Dependence of specific capacitance on current density. (e) Nyquist impedance plots of the supercapacitor. Inset is a magnified view of the high-frequency region. (f) Cycling stability of a solid-state device over 1000 cycles at a current density of 1 A g^{-1}. Inset shows the galvanostatic charge−discharge curves for the first 20 cycles.

the D and G bands is in accordance with the ratio of sp^3 to sp^2 carbon atoms, which can be used to derive information about the disordered and ordered domains of graphene.[50] As shown in Figure 4b, the value of the ratio of the intensity of peak D versus that of peak G (i.e., I_D/I_G) for CNF/RGO/CNT (i.e., 1.18) is higher than that of CNF/GONS/CNT (i.e., 1.01). This type of change in the value of I_D/I_G has previously been attributed to the generation of new sp^2 graphitic domains whose sizes are smaller and whose numbers are greater than those of the domains present in the GONSs before reduction.[50]

To gain further insight into the level of success of the thermal reduction of GONS in the CNF/GONS/CNT aerogel, X-ray photoelectron spectroscopy (XPS) was used to study the CNF/GONS/CNT aerogel before and after the thermal reduction process (Figure 5). The high-resolution XPS C1s spectrum of the CNF/GONS/CNT aerogel clearly indicated the presence of four types of carbon atoms in different functional groups: the nonoxygenated ring carbon (C═C/C−C, 284.4 eV), ether carbon (C−O, 286.2 eV), carbonyl carbon (C═O 287.8 eV), and carboxylate carbon (O−C═O, 289.2 eV).[50] The peak intensity of the C═C/C−C carbon in the CNF/RGO/CNT aerogel increased significantly compared to that of the CNF/GONS/CNT aerogel. This indicates that GONSs were effectively reduced during the thermal reduction process.[50] However, there were still a large number of oxygen-containing groups that originated mainly from CNFs in the aerogel.

The thermal stabilities of the CNF, CNF/GONS/CNT, and CNF/RGO/CNT aerogels were measured by a thermogravimetric analyzer (TGA) in nitrogen over the temperature range of 30−800 °C, and the data are shown in Figure 6. In Figure

DOI: 10.1021/am507999s
ACS Appl. Mater. Interfaces 2015, 7, 3263−3271

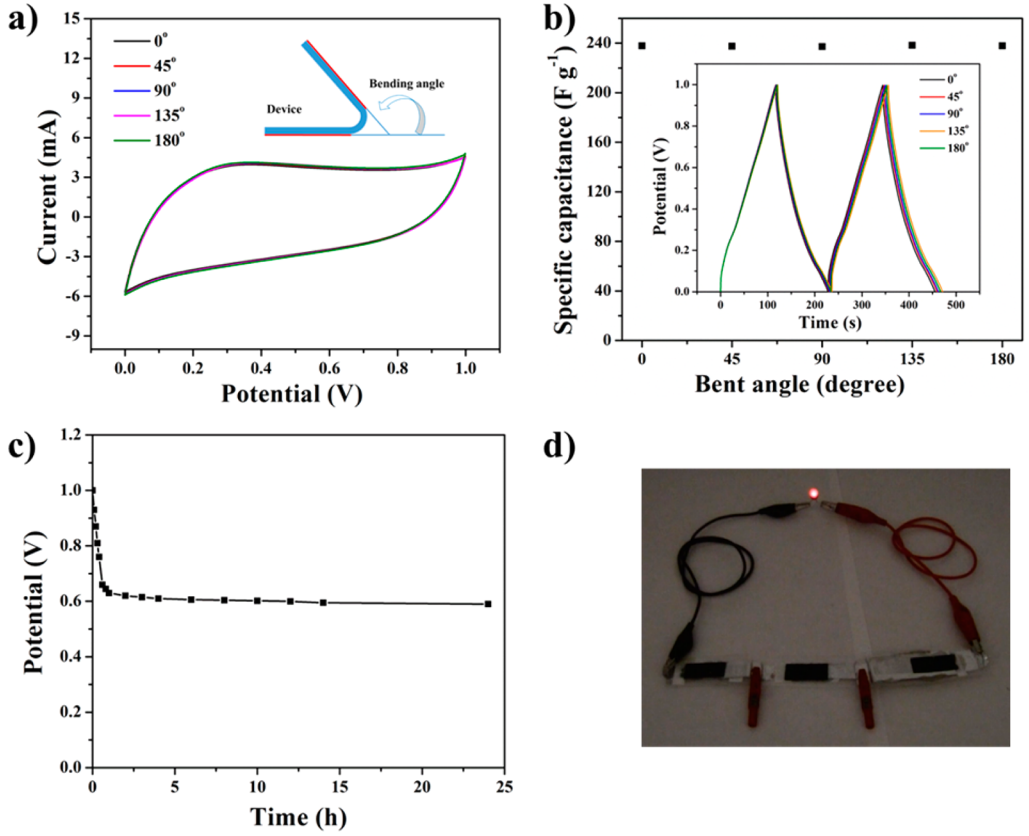

Figure 8. (a) Cyclic voltammetry curves of a supercapacitor at different bending angles with a scan rate of 10 mV S^{1-}. (b) Dependence of specific capacitance for a supercapacitor at different bending angles. The inset shows the charge−discharge curves of a supercapacitor at different bending angles with a current density of 1 A g^{-1}. (c) Self-discharge curves of a supercapacitor after being charged at 1.0 V for 10 min. (d) Three highly flexible devices used in series to light a red LED.

6b, the CNF/GONS/CNT aerogel shows two weight-loss processes. The weight loss that occurred over the temperature range of 144−226 °C was attributed to the loss of oxygen-containing groups from the GONSs.[50] The weight loss that occurred over the temperature range of 233−413 °C corresponded to the decomposition of CNFs in the CNF/GONS/CNT aerogel. This finding was validated by a comparison with the TGA curve of pure CNF aerogels.[32] There was only one weight-loss process shown in the TGA curve of the CNF/RGO/CNT aerogel, and it was associated with the decomposition of CNFs. These results led to the conclusion that the GONSs were successfully reduced to RGO.

Electrochemical Testing of Highly Flexible and All-Solid-State Supercapacitors. To show the superior performance of the CNF/RGO/CNT electrodes as electrochemical energy storage, the compressed CNF/RGO/CNT aerogel film was used to fabricate the supercapacitors without the use of any other binders, current collectors, or electroactive additives. Symmetric supercapacitors were assembled using a thin, flexible polyethylene terephthalate (PET) substrate and H_2SO_4/PVA gel as the electrolyte and separator (Figure 7a). The use of H_2SO_4/PVA-gel electrolytes reduced the thickness and weight of the electrode, as compared with aqueous electrolytes, and simplified the fabrication process because it did not require any special packing material. The electrochemical behavior of the electrode that was made from the CNF/RGO/CNT aerogel film was characterized via CV and galvanostatic charge−discharge testings. Figue 7b shows the CV curves of a supercapacitor device at various scan rates (5 to 50 mV s^{-1}) over a voltage range of 0−1 V. These curves showed a quasi-rectangular shape, suggesting that the compressed CNF/RGO/CNT aerogel film electrode exhibited an excellent electrical double-layer capacitive behavior[8] with a very rapid current response on voltage reversal and a low resistance of ion transport within the electrode. Figure 7c shows the nearly triangular and symmetrical shapes of the charge−discharge curves of such a device at various current densities. Figure 7d shows the specific electrode capacitances (i.e., C_{sp}) that were derived from the discharge curves. At a current density of 0.5 A g^{-1}, the C_{sp} of the supercapacitors was about 252 F g^{-1}, which was much higher than the C_{sp} of the assembled graphene paper[27,52,53] and carbon/cellulose composites (Table S1).[11,25,54] Previous studies demonstrated that the addition of conducting polymers could further increase the capacitances of the supercapacitors;[9,10,36,55,56] however, the lifetime of the carbon-/conducting polymer-based supercapacitors may be a concern. In addition, the supercapacitor made from the binder-free CNF/RGO/CNT electrodes showed an areal capacitance of 216 mF cm^{-2}, which is much higher than that recently reported for other types of flexible supercapacitor devices[11,25,54,57−59] (Table S2). When the current density was changed from 0.5 to 10 A g^{-1}, the supercapacitor retained 70% of its capacitance (177 A g^{-1}), indicating that the supercapacitor had an excellent capacitance retention capability resulting from the highly continuous porous structure and the strong hydrophlicity of the aerogel electrode that facilitated the diffusion of ions. Furthermore, these supercapacitors also showed an extremely high areal energy density of 28.4 μWh

DOI: 10.1021/am507999s
ACS Appl. Mater. Interfaces 2015, 7, 3263−3271

cm^{-2} (8.1 mWh g^{-1}) at an areal power density of 9.5 mW cm^{-2} (2.7 W g^{-1}); this was higher than the value recently reported for carbon-based supercapacitors.[25,54] The superior performance of the supercapacitors could be ascribed to several factors: (1) Graphene aggregation was effectively prevented by CNFs and perhaps also by CNTs. (2) The superior hydrophilic nature of the CNFs, present in the porous aerogel electrodes that exhibited a high specific surface energy, allowed excellent contact between the electrodes and the polymer-gel electrolyte, thereby providing diffusion channels for the electrolyte ions. (3) The incorporation of CNTs provided additional continuous conductive pathways between the different layers of graphene nanosheets.

The charge-transfer resistance (i.e., R_{ct}) and equivalent-series resistance (i.e., R_{ESR}) of the supercapacitors were characterized by electrochemical impedance spectroscopy (EIS). The Nyquist plots of the fabricated supercapacitor, recorded over the frequency range of 1 Hz to 100 kHz, are shown in Figure 7e. The Nyquist plot of a supercapacitor typically consists of a semicircle over the high-frequency range and a near vertical line over the low-frequency range.[60,61] However, the Nyquist plot of our supercapacitor did not have a semicircle at the high-frequency range, which is a desirable characteristic for supercapacitors. This finding may be attributed to the very small R_{ct} as well as the fact that the charge was stored mainly via a non-Faradaic process. The R_{ESR} of the supercapacitor was 10.5 Ω, and it was obtained from the intercept of the Nyquist plot with the real axis at high frequency. In the low-frequency range, the Nyquist plot of the supercapacitor was almost a vertical line, thus showing an ideal capacitive behavior. The fast ion diffusion in the CNF/RGO/CNT electrode was due to the highly porous microstructure and the superior wettability of the CNFs. The CNFs, which acted as electrolyte nanoreservoirs, provided good diffusion channels for electrolyte ions, enabling the active materials (i.e., RGO and CNTs) in the electrode to be in direct contact with the electrolyte, thus decreasing the distance the ions diffused.[25,62] As shown in the inset in Figure 7e, the enlarged plot of the high-frequency region showed that the supercapacitor displayed a pure capacitive behavior at frequencies up to ∼196 Hz.

The cyclic stability of the CNF/RGO/CNT electrodes, which is another important parameter for energy-storage devices, was evaluated by galvanostatic charge−discharge for 1000 cycles. Figure 7f provides the C_{sp} as a function of cycle number at a current density of 1 A g^{-1}. The C_{sp} of the supercapacitor remained nearly unchanged after 1000 charge−discharge cycles, suggesting that the supercapacitor made from the CNF/RGO/CNT electrode had superior cycle stability, which may be due to the interpenetrating structure formed between the electrodes and the polymer-gel electrolyte.[36] A typical charge−discharge curve under continuous operation for the first 20 cycles is shown in the inset of Figure 7f.

Future multifunctional energy-storage systems will require highly flexible devices[6] that can be easily rolled up. Therefore, electrochemical stability under bending is very important for all-solid-state flexible supercapacitors. Figure 8a shows the CV behavior of the supercapacitor tested under various bending angles. Bending did not cause any obvious effect on the capacitive performance. Figure8b shows the dependence of the specific capacitance of a supercapacitor fabricated from a compressed CNF/RGO/CNT aerogel film with an increasing bending angle from 0 to 180° at a current density of 1 A g^{-1}. The value of C_{sp} did not change notably with the increasing bending angle. More importantly, the shape of CV curve did not obviously change after withstanding 200 bending cycles (Figure S3), suggesting that these supercapacitors were highly flexible.

For practical applications, self-discharge of the device is one of the principal concerns. Figure 8c shows the self-discharge curves of a supercapacitor after it was charged at 1.0 V for 10 min. The voltage dropped significantly in the first several minutes; however, the self-discharge curve showed a plateau region after 1 h, with the potential decreasing very slowly. Nearly 59% of the initial charged potential was maintained even after 1 day, which was better than other reported values.[44,63] To demonstrate the use of the highly flexible and all-solid-state supercapacitor, three supercapacitor devices were assembled in series to light a red light-emitting diode (LED) with a minumum operating potential of 1.65 V. After being charged at a potential of 3.0 V, the device lit the LED very well for about 26 min (Figure 8d and Video S1).

CONCLUSIONS

A highly flexible and freestanding CNF/RGO/CNT aerogel electrode was synthesized by freeze-drying an aqueous dispersion of CNF/GONS/CNT, followed by the subsequent thermal reduction of GONSs in situ. All-solid-state flexible supercapacitors using compressed CNF/RGO/CNT aerogel film as the electrode exhibited a specific capacitance, energy density, and power density of 252 F g^{-1} (216 mF cm^{-2}), 8.1 mW h g^{-1} (28.4 μW h cm^{-2}), and 2.7 W g^{-1} (9.5 mW cm^{-2}), respectively. Moreover, the supercapacitors showed excellent cyclic stability, with more than 99.5% specific capacitance retained after 1000 charge−discharge cycles. Owing to its superior electrochemical performance, excellent process scalability, low cost, and environmentally friendliness, the CNF/RGO/CNT aerogel film may be a promising electrode material for assembling lightweight, flexible, low-cost, and rechargeable energy-storage devices.

ASSOCIATED CONTENT

Supporting Information

Preparation of cellulose nanofibril and graphene oxide, electrochemical calculation, SEM image of the cross-section of CNF/RGO/CNT film infiltrated with the gel electrolyte, CV test of a supercapacitor after 200 bending cycles, correlation between the specific capacitance and the scan rate, and comparison of the specific capacitance of the fabricated all-solid-state supercapacitor with other reported values. This material is available free of charge via the Internet at http://pubs.acs.org.

AUTHOR INFORMATION

Corresponding Author

*E-mail: sgong@engr.wisc.edu. Phone: +01 6083164311.

Notes

The authors declare no competing financial interest.

ACKNOWLEDGMENTS

The authors gratefully acknowledge the financial support of the University of Wisconsin−Madison and the USDA Forest Products Laboratory (Madison, WI).

DOI: 10.1021/am507999s
ACS Appl. Mater. Interfaces 2015, 7, 3263−3271

REFERENCES

(1) Nishide, H.; Oyaizu, K. Materials science - Toward flexible batteries. *Science* **2008**, *319*, 737−738.
(2) Nyholm, L.; Nystrom, G.; Mihranyan, A.; Stromme, M. Toward Flexible Polymer and Paper-Based Energy Storage Devices. *Adv. Mater. (Weinheim, Ger.)* **2011**, *23*, 3751−3769.
(3) Rogers, J. A.; Someya, T.; Huang, Y. G. Materials and Mechanics for Stretchable Electronics. *Science* **2010**, *327*, 1603−1607.
(4) Tarascon, J. M.; Armand, M. Issues and challenges facing rechargeable lithium batteries. *Nature* **2001**, *414*, 359−367.
(5) Liu, C.; Li, F.; Ma, L.-P.; Cheng, H.-M. Advanced Materials for Energy Storage. *Adv. Mater. (Weinheim, Ger.)* **2010**, *22*, E28−E62.
(6) Simon, P.; Gogotsi, Y. Materials for electrochemical capacitors. *Nat. Mater.* **2008**, *7*, 845−854.
(7) Wang, G.; Zhang, L.; Zhang, J. A review of electrode materials for electrochemical supercapacitors. *Chem. Soc. Rev.* **2012**, *41*, 797−828.
(8) Zhang, L. L.; Zhao, X. S. Carbon-based materials as supercapacitor electrodes. *Chem. Soc. Rev.* **2009**, *38*, 2520−2531.
(9) Chi, K.; Zhang, Z.; Xi, J.; Huang, Y.; Xiao, F.; Wang, S.; Liu, Y. Freestanding Graphene Paper Supported Three-Dimensional Porous Graphene−Polyaniline Nanocomposite Synthesized by Inkjet Printing and in Flexible All-Solid-State Supercapacitor. *ACS Appl. Mater. Interfaces* **2014**, *6*, 16312−16319.
(10) Shen, J.; Yang, C.; Li, X.; Wang, G. High-Performance Asymmetric Supercapacitor Based on Nanoarchitectured Polyaniline/Graphene/Carbon Nanotube and Activated Graphene Electrodes. *ACS Appl. Mater. Interfaces* **2013**, *5*, 8467−8476.
(11) Kang, Y. J.; Chun, S.-J.; Lee, S.-S.; Kim, B.-Y.; Kim, J. H.; Chung, H.; Lee, S.-Y.; Kim, W. All-Solid-State Flexible Supercapacitors Fabricated with Bacterial Nanocellulose Papers, Carbon Nanotubes, and Triblock-Copolymer Ion Gels. *ACS Nano* **2012**, *6*, 6400−6406.
(12) Liu, L.; Niu, Z.; Zhang, L.; Zhou, W.; Chen, X.; Xie, S. Nanostructured Graphene Composite Papers for Highly Flexible and Foldable Supercapacitors. *Adv. Mater. (Weinheim, Ger.)* **2014**, *26*, 4855−4862.
(13) Zhang, L. L.; Zhou, R.; Zhao, X. S. Graphene-based materials as supercapacitor electrodes. *J. Mater. Chem.* **2010**, *20*, 5983−5992.
(14) Tan, C.; Fung, B. M.; Newman, J. K.; Vu, C. Organic Aerogels with Very High Impact Strength. *Adv. Mater. (Weinheim, Ger.)* **2001**, *13*, 644−646.
(15) Sun, H.; Xu, Z.; Gao, C. Multifunctional, Ultra-Flyweight, Synergistically Assembled Carbon Aerogels. *Adv. Mater. (Weinheim, Ger.)* **2013**, *25*, 2554−2560.
(16) Geim, A. K.; Novoselov, K. S. The rise of graphene. *Nat. Mater.* **2007**, *6*, 183−191.
(17) Zhu, Y.; Murali, S.; Cai, W.; Li, X.; Suk, J. W.; Potts, J. R.; Ruoff, R. S. Graphene and Graphene Oxide: Synthesis, Properties, and Applications. *Adv. Mater. (Weinheim, Ger.)* **2010**, *22*, 3906−3924.
(18) Pumera, M. Graphene-based nanomaterials for energy storage. *Energy Environ. Sci.* **2011**, *4*, 668−674.
(19) Sun, Y.; Wu, Q.; Shi, G. Graphene based new energy materials. *Energy Environ. Sci.* **2011**, *4*, 1113−1132.
(20) Xu, C. H.; Xu, B. H.; Gu, Y.; Xiong, Z. G.; Sun, J.; Zhao, X. S. Graphene-based electrodes for electrochemical energy storage. *Energy Environ. Sci.* **2013**, *6*, 1388−1414.
(21) Han, S.; Wu, D.; Li, S.; Zhang, F.; Feng, X. Porous Graphene Materials for Advanced Electrochemical Energy Storage and Conversion Devices. *Adv. Mater. (Weinheim, Ger.)* **2014**, *26*, 849−864.
(22) You, B.; Jiang, J.; Fan, S. Three-Dimensional Hierarchically Porous All-Carbon Foams for Supercapacitor. *ACS Appl. Mater. Interfaces* **2014**, *6*, 15302−15308.
(23) Zhang, Z.; Xiao, F.; Guo, Y.; Wang, S.; Liu, Y. One-Pot Self-Assembled Three-Dimensional TiO_2-Graphene Hydrogel with Improved Adsorption Capacities and Photocatalytic and Electrochemical Activities. *ACS Appl. Mater. Interfaces* **2013**, *5*, 2227−2233.
(24) Zhang, Z.; Xiao, F.; Qian, L.; Xiao, J.; Wang, S.; Liu, Y. Facile Synthesis of 3D MnO_2−Graphene and Carbon Nanotube−Graphene Composite Networks for High-Performance, Flexible, All-Solid-State Asymmetric Supercapacitors. *Adv. Energy Mater.* **2014**, *4*, 1400064.
(25) Gao, K.; Shao, Z.; Li, J.; Wang, X.; Peng, X.; Wang, W.; Wang, F. Cellulose nanofiber-graphene all solid-state flexible supercapacitors. *J. Mater. Chem. A* **2013**, *1*, 63−67.
(26) Su, F.; Poh, C. K.; Chen, J. S.; Xu, G.; Wang, D.; Li, Q.; Lin, J.; Lou, X. W. Nitrogen-containing microporous carbon nanospheres with improved capacitive properties. *Energy Environ. Sci.* **2011**, *4*, 717−724.
(27) Yang, X.; Zhu, J.; Qiu, L.; Li, D. Bioinspired Effective Prevention of Restacking in Multilayered Graphene Films: Towards the Next Generation of High-Performance Supercapacitors. *Adv. Mater. (Weinheim, Ger.)* **2011**, *23*, 2833−2838.
(28) Klemm, D.; Heublein, B.; Fink, H.-P.; Bohn, A. Cellulose: Fascinating Biopolymer and Sustainable Raw Material. *Angew. Chem., Int. Ed.* **2005**, *44*, 3358−3393.
(29) Klemm, D.; Kramer, F.; Moritz, S.; Lindstrom, T.; Ankerfors, M.; Gray, D.; Dorris, A. Nanocelluloses: A New Family of Nature-Based Materials. *Angew. Chem., Int. Ed.* **2011**, *50*, 5438−5466.
(30) Moon, R. J.; Martini, A.; Nairn, J.; Simonsen, J.; Youngblood, J. Cellulose nanomaterials review: structure, properties and nanocomposites. *Chem. Soc. Rev.* **2011**, *40*, 3941−3994.
(31) Chen, W.; Yu, H.; Li, Q.; Liu, Y.; Li, J. Ultralight and highly flexible aerogels with long cellulose I nanofibers. *Soft Matter* **2011**, *7*, 10360−10368.
(32) Javadi, A.; Zheng, Q.; Payen, F.; Javadi, A.; Altin, Y.; Cai, Z.; Sabo, R.; Gong, S. Polyvinyl Alcohol-Cellulose Nanofibrils-Graphene Oxide Hybrid Organic Aerogels. *ACS Appl. Mater. Interfaces* **2013**, *5*, 5969−5975.
(33) Sehaqui, H.; Zhou, Q.; Berglund, L. A. High-porosity aerogels of high specific surface area prepared from nanofibrillated cellulose (NFC). *Compos. Sci. Technol.* **2011**, *71*, 1593−1599.
(34) Zheng, Q.; Cai, Z.; Gong, S. Green synthesis of polyvinyl alcohol (PVA)-cellulose nanofibril (CNF) hybrid aerogels and their use as superabsorbents. *J. Mater. Chem. A* **2014**, *2*, 3110−3118.
(35) Bao, L. H.; Li, X. D. Towards Textile Energy Storage from Cotton T-Shirts. *Adv. Mater. (Weinheim, Ger.)* **2012**, *24*, 3246−3252.
(36) Li, S.; Huang, D.; Zhang, B.; Xu, X.; Wang, M.; Yang, G.; Shen, Y. Flexible Supercapacitors Based on Bacterial Cellulose Paper Electrodes. *Adv. Energy Mater.* **2014**, *4*, 1301655.
(37) Bordjiba, T.; Mohamedi, M.; Dao, L. H. New Class of Carbon-Nanotube Aerogel Electrodes for Electrochemical Power Sources. *Adv. Mater. (Weinheim, Ger.)* **2008**, *20*, 815−819.
(38) Futaba, D. N.; Hata, K.; Yamada, T.; Hiraoka, T.; Hayamizu, Y.; Kakudate, Y.; Tanaike, O.; Hatori, H.; Yumura, M.; Iijima, S. Shape-engineerable and highly densely packed single-walled carbon nanotubes and their application as super-capacitor electrodes. *Nat. Mater.* **2006**, *5*, 987−994.
(39) Cote, L. J.; Kim, J.; Tung, V. C.; Luo, J. Y.; Kim, F.; Huang, J. X. Graphene oxide as surfactant sheets. *Pure Appl. Chem.* **2011**, *83*, 95−110.
(40) Kim, J.; Cote, L. J.; Kim, F.; Yuan, W.; Shull, K. R.; Huang, J. X. Graphene Oxide Sheets at Interfaces. *J. Am. Chem. Soc.* **2010**, *132*, 8180−8186.
(41) Adsul, M. G.; Rey, D. A.; Gokhale, D. V. Combined strategy for the dispersion/dissolution of single walled carbon nanotubes and cellulose in water. *J. Mater. Chem.* **2011**, *21*, 2054−2056.
(42) Zheng, Q.; Javadi, A.; Sabo, R.; Cai, Z.; Gong, S. Polyvinyl alcohol (PVA)-cellulose nanofibril (CNF)-multiwalled carbon nanotube (MWCNT) hybrid organic aerogels with superior mechanical properties. *RSC Adv.* **2013**, *3*, 20816−20823.
(43) Wei, H. G.; Gu, H. B.; Guo, J.; Wei, S. Y.; Guo, Z. H. Electropolymerized Polyaniline Nanocomposites from Multi-Walled Carbon Nanotubes with Tuned Surface Functionalities for Electrochemical Energy Storage. *J. Electrochem. Soc.* **2013**, *160*, G3038−G3045.
(44) Meng, C.; Liu, C.; Chen, L.; Hu, C.; Fan, S. Highly Flexible and All-Solid-State Paperlike Polymer Supercapacitors. *Nano Lett.* **2010**, *10*, 4025−4031.
(45) Chandrasekaran, R.; Soneda, Y.; Yamashita, J.; Kodama, M.; Hatori, H. Preparation and electrochemical performance of activated carbon thin films with polyethylene oxide-salt addition for electro-

DOI: 10.1021/am507999s
ACS Appl. Mater. Interfaces 2015, 7, 3263−3271

chemical capacitor applications. *J. Solid State Electrochem.* **2008**, *12*, 1349−1355.
(46) Okita, Y.; Saito, T.; Isogai, A. Entire Surface Oxidation of Various Cellulose Microfibrils by TEMPO-Mediated Oxidation. *Biomacromolecules* **2010**, *11*, 1696−1700.
(47) Tonoli, G. H. D.; Teixeira, E. M.; Corrêa, A. C.; Marconcini, J. M.; Caixeta, L. A.; Pereira-da-Silva, M. A.; Mattoso, L. H. C. Cellulose micro/nanofibres from Eucalyptus kraft pulp: Preparation and properties. *Carbohydr. Polym.* **2012**, *89*, 80−88.
(48) Compton, O. C.; Jain, B.; Dikin, D. A.; Abouimrane, A.; Amine, K.; Nguyen, S. T. Chemically Active Reduced Graphene Oxide with Tunable C/O Ratios. *ACS Nano* **2011**, *5*, 4380−4391.
(49) Wang, G.; Shen, X.; Wang, B.; Yao, J.; Park, J. Synthesis and characterisation of hydrophilic and organophilic graphene nanosheets. *Carbon* **2009**, *47*, 1359−1364.
(50) Stankovich, S.; Dikin, D. A.; Piner, R. D.; Kohlhaas, K. A.; Kleinhammes, A.; Jia, Y.; Wu, Y.; Nguyen, S. T.; Ruoff, R. S. Synthesis of graphene-based nanosheets via chemical reduction of exfoliated graphite oxide. *Carbon* **2007**, *45*, 1558−1565.
(51) Wu, H.; Zhao, W.; Hu, H.; Chen, G. One-step *in situ* ball milling synthesis of polymer-functionalized graphene nanocomposites. *J. Mater. Chem.* **2011**, *21*, 8626−8632.
(52) Yu, A.; Roes, I.; Davies, A.; Chen, Z. Ultrathin, transparent, and flexible graphene films for supercapacitor application. *Appl. Phys. Lett.* **2010**, *96*, 253105.
(53) Liu, F.; Song, S.; Xue, D.; Zhang, H. Folded Structured Graphene Paper for High Performance Electrode Materials. *Adv. Mater. (Weinheim, Ger.)* **2012**, *24*, 1089−1094.
(54) Weng, Z.; Su, Y.; Wang, D.-W.; Li, F.; Du, J.; Cheng, H.-M. Graphene−Cellulose Paper Flexible Supercapacitors. *Adv. Energy Mater.* **2011**, *1*, 917−922.
(55) Wang, D.-W.; Li, F.; Zhao, J.; Ren, W.; Chen, Z.-G.; Tan, J.; Wu, Z.-S.; Gentle, I.; Lu, G. Q.; Cheng, H.-M. Fabrication of Graphene/Polyaniline Composite Paper via In Situ Anodic Electropolymerization for High-Performance Flexible Electrode. *ACS Nano* **2009**, *3*, 1745−1752.
(56) Zhang, K.; Zhang, L. L.; Zhao, X. S.; Wu, J. Graphene/Polyaniline Nanofiber Composites as Supercapacitor Electrodes. *Chem. Mater.* **2010**, *22*, 1392−1401.
(57) Chen, J.; Sheng, K.; Luo, P.; Li, C.; Shi, G. Graphene Hydrogels Deposited in Nickel Foams for High-Rate Electrochemical Capacitors. *Adv. Mater. (Weinheim, Ger.)* **2012**, *24*, 4569−4573.
(58) Hu, L.; Choi, J. W.; Yang, Y.; Jeong, S.; La Mantia, F.; Cui, L.-F.; Cui, Y. Highly conductive paper for energy-storage devices. *Proc. Natl. Acad. Sci. U.S.A.* **2009**, *51*, 21490−21494.
(59) Pasta, M.; La Mantia, F.; Hu, L.; Deshazer, H.; Cui, Y. Aqueous supercapacitors on conductive cotton. *Nano Res.* **2010**, *3*, 452−458.
(60) Wang, G.; Sun, X.; Lu, F.; Sun, H.; Yu, M.; Jiang, W.; Liu, C.; Lian, J. Flexible Pillared Graphene-Paper Electrodes for High-Performance Electrochemical Supercapacitors. *Small* **2012**, *8*, 452−459.
(61) Yuan, L.; Xiao, X.; Ding, T.; Zhong, J.; Zhang, X.; Shen, Y.; Hu, B.; Huang, Y.; Zhou, J.; Wang, Z. L. Paper-Based Supercapacitors for Self-Powered Nanosystems. *Angew. Chem., Int. Ed.* **2012**, *51*, 4934−4938.
(62) Gui, Z.; Zhu, H.; Gillette, E.; Han, X.; Rubloff, G. W.; Hu, L.; Lee, S. B. Natural Cellulose Fiber as Substrate for Supercapacitor. *ACS Nano* **2013**, *7*, 6037−6046.
(63) Ganesh, B.; Kalpana, D.; Renganathan, N. G. Acrylamide based proton conducting polymer gel electrolyte for electric double layer capacitors. *Ionics* **2008**, *14*, 339−343.

DOI: 10.1021/am507999s
ACS Appl. Mater. Interfaces 2015, 7, 3263−3271